

# Thermal Characterization of Smart and Large-Scale Building Envelope System in a Subtropical Climate

Andrey A. Chernousov, Ben Y. B. Chan

**Abstract**—The thermal behavior of a large-scale, phase change material (PCM) enhanced building envelope system was studied in regard to the need for pre-fabricated construction in subtropical regions. The proposed large-scale envelope consists of a reinforced aluminum skin, insulation core, phase change material and reinforced gypsum board. The PCM impact on an energy efficiency of an enveloped room was resolved by validation of the EnergyPlus numerical scheme and optimization of a smart material location in the core. The PCM location was optimized by a minimization method of a cooling energy demand. It has been shown that there is good agreement between the test and simulation results. The optimal location of the PCM layer in Hong Kong summer conditions has been then recomputed for core thicknesses of 40, 60 and 80 mm. A non-dimensional value of the optimal PCM location was obtained to be same for all the studied cases and the considered external and internal conditions.

**Keywords**—Thermal performance, phase change material, energy efficiency, PCM optimization.

## I. INTRODUCTION

PRE-FABRICATED large-scale building envelopes, with polymer foam cores laminated by metallic or fiber reinforced polymer (FRP), form part of energy efficient and economical structures [1], [2]. They have many attractive features, such as high strength-to-weight ratio, fast erectability, transportability, pre-fabricability, durability and recyclability. In order to improve the thermal mass of lightweight sandwiches in an economical manner, in relation to the daily cooling load balancing, phase change materials (PCMs) can be applied [3]. As a result, the daily cooling energy load is more uniform, like in the case when using much heavier pre-cast concrete. Thus, the smart lightweight sandwich approach is very attractive in hot subtropical climates [4]–[6]. For the modeling of lightweight multilayered envelopes, the EnergyPlus software is commonly used. It enables the accurate estimation of the PCM layer behavior in the designing of multilayered structures.

Cheung et al. have reported on a smart sandwich system with the PCM placed near the interior skin, i.e. close to the indoor condition controlled by the cooling system [7]. The PCM layer was supposed to be charged and discharged maximally during the summer season as the PCM melting point  $T_{mp}$  agreed with the maintained indoor temperature. As a result, the off-peak (10 pm - 7 am) cooling energy consumption was increased from

28 to 44%. Despite successful attempts in the development of the above mentioned building envelopes, certain questions have not been answered. It remains unclear that if the PCM layer is at its optimal position in the insulation core. Moreover, the developed thermal model for the envelope has not yet been validated in a full-scale laboratory test, under real weather loads existing in the subtropical region.

This paper reports the continuation of existing achievements and is part and parcel of the development of large-scale and smart building envelopes for subtropical regions.

## II. THE ENVELOPE SYSTEM DESCRIPTION

The overall size of a typical large-scale envelope system is 3 m × 3 m, and is aimed for typical floor to floor heights. A schematic section of the system is given in Fig. 1. A skin of aluminum (A) is placed in series with an exterior basalt fiber reinforced polymer (B) and polyisocyanurate foam (C). This is followed by a PCM (D), interior BFRP (E) and finished layer of gypsum board (F). The relatively thin layer of PCM and aluminum container cause melting of the entire smart material almost simultaneously.

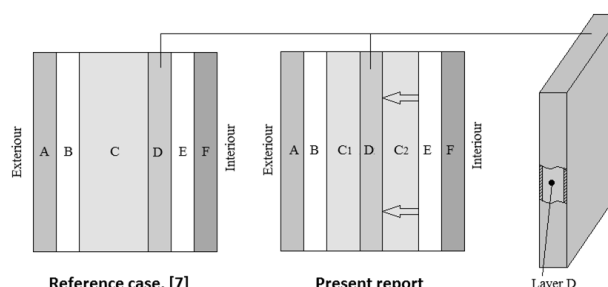


Fig. 1 PCM location changing in the smart building envelope system

Table I gives some measured properties for the constituent layers used in the modeling. The layer thickness  $t$  was measured by a IP65 digital micrometer (Series M18). The hot wire method (QTM-500, KYM Co., Ltd.) and the DSC method of ASTM E1269 (Q1000, TA Instruments) were respectively used for thermal conductivity  $k$  and specific heat capacity  $c_p$  measurement. The material density  $d$  was determined as the ratio of mass to volume of the measured material. The thermal mass per  $m^2$  of panel was calculated by (1):

$$C = d \cdot V \cdot c_p \quad (1)$$

where the  $V$  is the volume.

Commercially available PCM was bought in the Rubitherm Shijiazhuang PCMs Company and labeled as the PCM-C. Its

A. A. Chernousov is with the Department of Civil and Environmental Engineering, Hong Kong University of Science and Technology, Hong Kong, HKSAR, China (phone: +852 90735889; e-mail: chernous@ust.hk).

B. Y. B. Chan is with the Department of Civil and Environmental Engineering, Hong Kong University of Science and Technology, Hong Kong, HKSAR, China (e-mail: ybchan@ust.hk).

density changes from 0.85 to 0.82 g/cm<sup>3</sup> after complete melting. In a comparison, the PCM-C differs from the reference PCM [7], [8]. It has the same thermal conductivity of around 0.2 W/(m·K), but different phase change intervals. Fig. 2 shows the enthalpy  $\Delta H$  variations as a function of temperature  $T$  for the PCMs. The PCM-C accumulates around 200 J/g by its total melting from 26 to 35°C. As mentioned, the effect of PCM replacement can be compensated by changing its location in the insulation core (Fig. 1).

TABLE I  
COMPOSITION AND MATERIAL PROPERTIES OF THE ENVELOPE

Material	$t$ (mm)	$k$ (W/mK)	$c_p$ (J/gK)	$d$ (kg/m <sup>3</sup> )	$C$ (kJ/K)
A Aluminum	0.5-5	201	0.88	2700	1.2-12
B Ext. BFRP	2	0.35	0.75	1660	2.5
C PIR	40-80	0.033	1.32	45	2.4-4.8
D PCM-C	2.5	0.2	3.49	849	7.4
E Int. BFRP	2	0.35	0.75	1660	2.5
F Gypsum	12	0.16	1.15	640	8.8

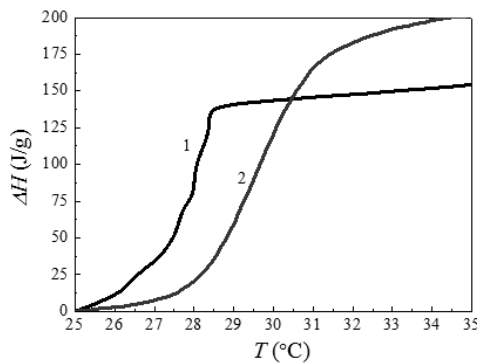


Fig. 2 Temperature function of an enthalpy for the PCM-C (curve 2) and the reference PCM [7] (curve 1)

### III. ENERGY PLUS PCM MODEL

An implicit finite difference scheme is used in EnergyPlus 7.2 [9], where a fully implicit (1<sup>st</sup> order) or semi-implicit Crank-Nicolson scheme (2<sup>nd</sup> order) may be chosen. Equations (2.1) and (2.2) show the computation method of the Crank-Nicolson scheme inside the sandwich layer system.

$$c_p \cdot d \cdot \Delta X (T_i^{j+1} - T_i^j) / \Delta t = 0.5 \cdot k_w \cdot (T_{i+1}^{j+1} - T_i^{j+1}) / \Delta X + 0.5 \cdot k_E \cdot (T_{i-1}^{j+1} - T_i^{j+1}) / \Delta X + 0.5 \cdot k_w \cdot (T_{i+1}^j - T_i^j) / \Delta X + 0.5 \cdot k_E \cdot (T_{i-1}^j - T_i^j) / \Delta X \quad (2.1)$$

$$k_w = 0.5 \cdot (k_{i+1}^{j+1} - k_i^{j+1}), \quad k_E = 0.5 \cdot (k_{i-1}^{j+1} - k_i^{j+1}) \quad (2.2)$$

where  $k_i = k_i(T)$  if the thermal conductivity is variable,  $T$  is temperature,  $i$  is a node being modeled,  $i+1$  is an adjacent node to the interior,  $i-1$  is an adjacent node to the exterior,  $j+1$  is a new time step,  $j$  is a previous time step,  $\Delta\tau$  is a time step,  $\Delta X$  is a finite difference layer thickness,  $c_p$  is the material specific heat capacity, and  $d$  is the material density.

The finite difference layer thickness is computed by (3), where  $a$  is the thermal diffusivity of the material and  $Fo$  is the Fourier number.

$$\Delta X = \sqrt{a \cdot \Delta\tau / Fo} \quad (3)$$

The described algorithm is combined with the enthalpy-temperature function. Because of the iteration scheme used, the nodal enthalpies are updated at each iteration step, and then they are used to develop the value of  $c_p$ .

$$c_p = (H_i^{j+1} - H_i^j) / (T_i^{j+1} - T_i^j) \quad (4)$$

### IV. VERIFICATION AND VALIDATION OF ENERGYPLUS SCHEME

#### A. Experimental Setup and Boundary Conditions

In order to verify and determine the thermal efficiency of the designed panels, the numerical model should match the laboratory test results for a certain period. The period from 22<sup>nd</sup> to 25<sup>th</sup> of July was chosen in accordance with weather data of a typical meteorological year (TMY) [10].

The PCM integrated sandwich, 100 mm thick, was chosen as a test sample, with a 3 mm facing of AA 5005 and 80 mm of PIR, which provide excellent protection against intense solar irradiation and heat transfer through the insulation, respectively. The sample used in the experiments had overall dimension of 0.9 m × 0.9 m. A series of preliminary tests have shown that 80 mm of PIR foam does not allow the accurate temperature measurement of PCM as it has a relatively high thermal resistance. A solution is to have the PCM closer to the skin surface. After validation of such an E+ model, the optimal location of PCM may be simply computed. The sample scheme, given in Fig. 3, was selected for the validation test.

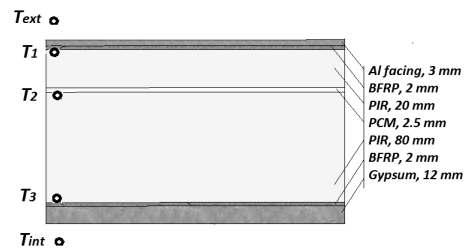


Fig. 3 Test wall configuration with dimensions and location of temperature sensors

A diagram and general view of the experimental facilities are shown in Fig. 4. The test sample was installed in a hot box, made of PIR. The internal dimensions of the hot box are 0.9 m × 0.9 m × 0.5 m with a wall thickness of 0.13 m. For the sunshine simulator, there are 4 halogen lamps (ED401 R7s, Everspring Ind. Co) integrated with a programmable autotransformer and power supply.

As seen from Fig. 4, the measured temperatures  $T_1$ ,  $T_2$  and  $T_3$  were collected, whilst  $T_{ext}$  was maintained according to the Hong Kong TMY data, and  $T_{int}$  was set as 25 °C. The test was conducted inside an environmental chamber at the Jockey Club Controlled Environment Test Facility in the Department of Mechanical Engineering of HKUST.

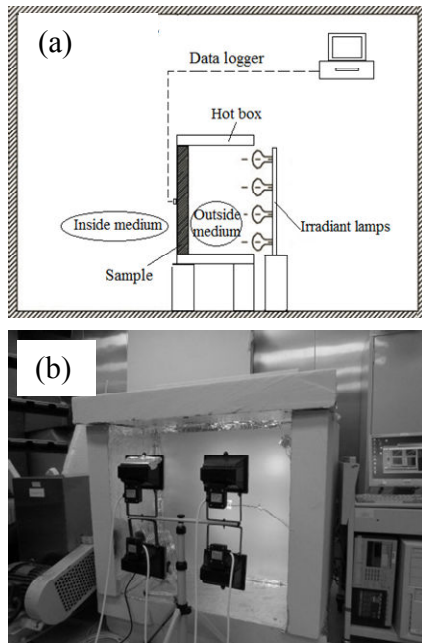


Fig. 4 Diagram (a) and general view (b) of the validation test inside the chamber with controllable conditions

#### B. Validation Results of the Sample Thermal Behavior

The proposed numerical model from E+ was verified by comparing the simulation and experimental results. The initial temperatures of the sample layers were in the range of 25-25.4°C. The entire time of the testing was about 90 hours. First of all, the outside surface temperature  $T_1$ , as given in Fig. 5, represents a good agreement between the curves with peak temperatures of about 37-38°C. The  $T_1$  distribution is a determining factor for the temperature validation of the subsequent layers.

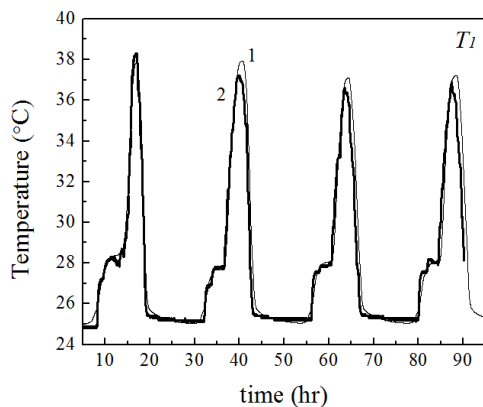


Fig. 5 Comparison of simulated (1) and experimental results (2) for the outside surface temperature  $T_1$

Fig. 6 compares the results for temperatures  $T_2$  and  $T_3$ . As is seen in Fig. 6, there is obvious shifting between the curves. The experimental values for  $T_2$  and  $T_3$  typically lag the simulated results by 0.6 hr and 2 hr, respectively. Moreover, the error increases day by day, while the lines have almost a similar behavior and values. The maximum temperature difference is

not more than 1°C (3.8%) for the phase change material  $T_2$  and 0.7°C (2.8%) for the  $T_3$  temperature.

The experiments carried out show that an effective, validated numerical model for the multilayered system with PCM was obtained. Thus, it is possible to apply the validated scheme on a long term simulation. The optimal PCM location will be computed for different room temperatures of 22 or 26°C and different insulator thicknesses of 40, 60 and 80 mm.

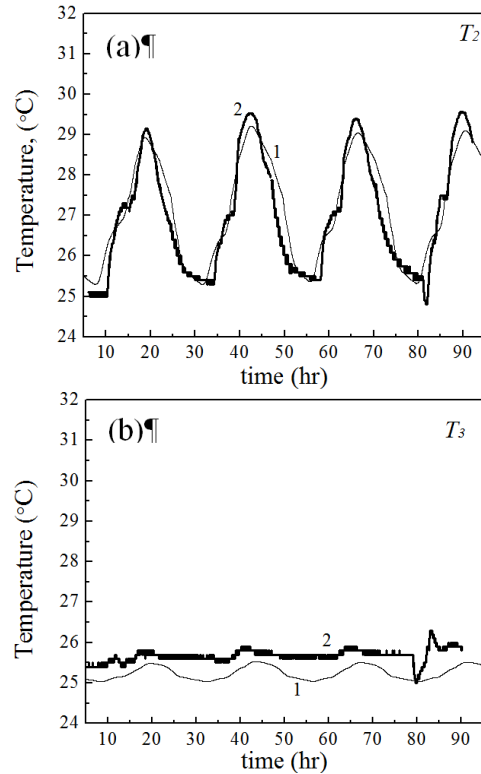


Fig. 6 Comparisons of simulated (1) and experimental results (2) for the temperatures of  $T_2$  (a) and  $T_3$  (b)

#### V. PCM OPTIMIZATION

For the PCM optimization, an approach using the optimum PCM position inside the foam insulator is chosen. The PCM-container is shifted from the B layer to E layer, defined by relative parameter of  $x$ :

$$x = t_{C1} / (t_{C1} + t_{C2}) \quad (7)$$

where  $t_{C1}$  and  $t_{C2}$  are the thicknesses of the exterior and interior core part, respectively. Hence, in the PCM shifting,  $x$  changes from 0 (ext. BFRP) to 1 (int. BFRP). The PCM shifting affects the on-time cooling energy demand  $Q_{on}$  of the room against the heat penetrating through the envelope. As a percentage, the PCM efficiency can be evaluated by:

$$Q_{on} = \sum_{\tau} Q_{on} / \left( \sum_{\tau} Q_{on} + \sum_{\tau} Q_{off} \right) \cdot 100\% \quad (8)$$

where  $\sum Q_{on}$  and  $\sum Q_{off}$  are the total on-peak and off-peak energy demanded by a building air conditioning to maintain a desired

temperature,  $\tau$  is the simulation time period from the 1<sup>st</sup> of May to the 30<sup>th</sup> of October. Temporal coverage of  $Q_{on}$  may be different for different cities, but it was fixed as 7 am-10 pm in subtropical regions. Moreover,  $Q_{on}$  is computed according to the TMY Hong Kong data for a period from 1<sup>st</sup> May to 30<sup>th</sup> October. During the simulation period, the room temperature was maintained at 22°C or 26°C. Thus, the optimization problem narrows to searching for the most suitable shifting of the 2.5 mm PCM layer within the interval of 22-26°C.

Table II illustrates the composition of the optimized envelopes, with external dimensions of 3 m×3 m. The cooling energy demand  $Q_{TOTAL}$  for the 9 m<sup>2</sup> envelopes  $E_A$ ,  $E_B$  and  $E_C$  ranges from 112 to 275 kWh.

TABLE II  
 COMPOSITION OF OPTIMIZED MULTILAYERED ENVELOPES (9M<sup>2</sup>) AND THEIR INFLUENCE ON TOTAL ENERGY DEMAND

Envelope case	t (mm)						Q <sub>TOTAL</sub> (kWh)	
	A	B	C	D	E	F	22 °C	26 °C
E <sub>A</sub>	3	2	40	2.5	2	12	275	182
E <sub>B</sub>	3	2	60	2.5	2	12	208	138
E <sub>C</sub>	3	2	80	2.5	2	12	168	112

The optimization results are illustrated in Fig. 7, 8. All the dependences represent parabolic lines with  $Q_{on}(E_A) > Q_{on}(E_B) > Q_{on}(E_C)$  and a blurred minimum around 60%. These values correspond to the  $Q_{on}$  minima for the panels with  $t_C = 80-130$  mm and  $t_D = 0-10$  mm in the same simulation conditions [7].

The optimal shifting  $x_{opt}$  for 22 °C ranges from 0.5 to 0.7, but when the maintained room temperature is 26 °C, the  $x_{opt}$  drifts to the interval of 0.7-0.85. The community of the results suggests that  $x_{opt}$  is around 0.7 for all the studied cases.

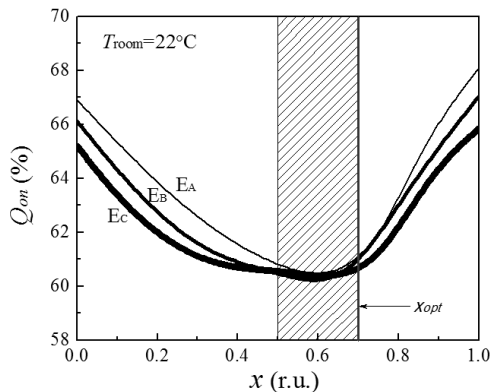


Fig. 7 Influence of a PCM location changing  $x$  on the  $Q_{on}$  of the enveloped room with the maintained temperature of 22°C

That is the  $t_{C1}/t_{C2}$  ratios are 28 mm/12 mm, 42 mm/18 mm and 56 mm/24 mm for the 40, 60 and 80 mm insulation cores, respectively.

It should be noted also that the admissible deviation in the PCM location is 4-5% because of the blurred minima in the results.

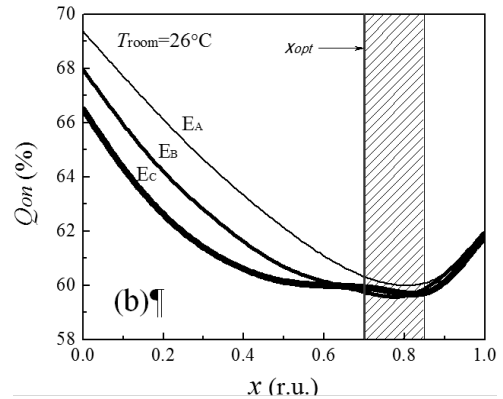


Fig. 8 Influence of a PCM location changing  $x$  on the  $Q_{on}$  of the enveloped room with the maintained temperature of 26°C

## VI. CONCLUSION

Using the lightweight, large-scale and smart building envelope system is a very promising solution to cut electricity expenses in the subtropical regions. This system can contain paraffinic PCM with various thermal characteristics, however, it is recommended to optimize the proposed PCM by shifting its location in the insulation core. As shown in the Hong Kong weather conditions, an optimal location of PCM can be found for the maintained room temperature range of 22-26°C and the core thickness range of 40-80 mm. This means that the energy efficiency is almost the same for all the optimized systems.

The optimization approach was based on the envelope material chosen and the numerical scheme validation of the PCM enhanced system ( $t_D = 2.5$  mm) with the 80 mm insulation thick. The comparison of the test and simulated temperatures in the panel layers showed satisfactory agreement. The envelopes with the insulation thicknesses of 40, 60 and 80 mm were optimized by the method of the cooling energy demand minimization. The optimal PCM position was found to be shifted by the same non-dimensional value  $x = 0.7$  for all the considered cases. That is the  $t_{C1}/t_{C2}$  ratios are 28 mm/12 mm, 42 mm/18 mm and 56 mm/24 mm for the 40, 60 and 80 mm of insulation core, respectively.

## ACKNOWLEDGMENT

The work described in this paper was fully supported by UC RUSAL as part of the funded research on the development of large-scale pre-insulated fiber reinforced aluminum envelopes and cantilevered roof systems.

## REFERENCES

- [1] J. M. Davies, *Lightweight sandwich construction*. Oxford: Blackwell Science, 2001, 384 p.
- [2] R. Koschade, *Sandwich Panel Construction: Construction with factory engineered sandwich panels, consisting of metallic facings and a foamed polyurethane core*, Weinheim, Wiley, 2002, 390 p.
- [3] S. Raoux, M. Wuttig, *Phase Change Materials*, Boston, Springer US, 2009, 430 p.
- [4] C. A. Balaras, "The role of thermal mass on the cooling load of buildings: An overview of computational methods", *Energy and Buildings*, vol. 24 (1), pp. 1-10, 1996.
- [5] C.K. Halford, R. F. Boeh, "Modeling of phase change material peak load shifting, *Energy and Buildings*", vol. 39, pp. 298-330, March 2007.

- [6] A. Tardieu, S. Behzadi, J. J. J. Chen and M. M. Farid, "Computer simulation and experimental measurements for an experimental PCM-integrated office building", in: *12th Conf. Int. Building Performance Simulation Association*, Sydney, 2011, pp. 56–63.
- [7] M. M. S. Cheung, A. A. Chernousov, B. Y. B. Chan and P. Wang, "Thermal performance of large-scale pre-insulated building envelope in Hong Kong", in: *6th ECCOMAS Thematic Conf. on Smart Structures and Materials*, Turin, 2013.
- [8] P. Losada-Pérez et al., "Measurements of Heat Capacity and Enthalpy of Phase Change Materials by Adiabatic Scanning Calorimetry", *Int. J. of Thermophysics*, vol. 32, pp. 913–924, May 2011.
- [9] U.S. Department of Energy Home page, <http://apps1.eere.energy.gov/buildings/energyplus/pdfs/engineeringreference.pdf>, 2013 (accessed September 20, 2013).
- [10] A. L. S. Chan, T. T. Chow, S. K. F. Fong and J. Z. Lin, "Generation of a typical meteorological year for Hong Kong", *Energy Conversion and Management*, vol. 83, pp. 87–96, Jan. 2006.